European Geothermal Congress 2013
Pisa, Italy, 3-7 June 2013

Non-stationary seismic hazard evaluation for gas fields in The Netherlands

Mauro Caccavale[1], Torild van Eck[1], Bernard Dost[1], Dirk Kraaijpoel[1]

[1] Seismology Division KNMI (Royal Netherlands Meteorological Institute)
Address PO Box 201 NL-3730 AE De Bilt, Netherlands

mauro.caccavale@knmi.nl

Keywords: seismic hazard, induced seismicity, non-stationary seismic hazard, gas exploration.

ABSTRACT

The seismic hazard due to induced seismicity was evaluated for gas fields where a time-depended seismicity was identified. This analysis was performed using a classical Probabilistic Seismic Hazard Analysis (PSHA) (Cornell, 1968) approach. The PSHA allows defining the state-of-art of current knowledge with regard to about 20 years of induced seismicity. On the other hand a classical PSHA approach is based on a stationary Poisson model probably not appropriate to describe the time varying induced seismicity. To overcome this limitation it is possible to define different time windows in which the stationary hypothesis is still valid or use a more general/complex approach using a non-stationary Poisson model. The second option is substituting the constant activity seismicity rate (λ) with a time dependent variable ($\lambda(t)$). Both approaches were investigated using seismicity data from exploration fields in The Netherlands.

1. INTRODUCTION

Exploitation of subsurface energy resources within populated areas may have large economic and social implications. One of the major social impacts is the occurrence of earthquakes, which may be induced by subsurface activities such as gas production/storage, mining and geothermal energy retrieval Although the magnitudes are usually moderate, the shallow depth makes these events perceptible and potentially damaging (Basel, Larderello, Groningen). The socio-economic aspect requires guarding the population and infrastructure (roads, factory, pipelines …) from nuisance, damage and possible injuries. For this purpose the EC project GEISER is developing a different methodology to improve our knowledge and models to describe, forecast and mitigate induced seismicity. In the framework of this project different studies approached/evaluated temporal variation of the anthropogenic seismic hazard.

The gas reservoir field of Groningen is one of the larger gas reservoir in the world and certainly of significant importance in the Dutch energy and economy. Induced seismicity has been reported since 1986 and is monitored by a network of borehole seismometers and accelerometers at the surface, which has been upgraded and extended during the last years. Since 1991 and up to February 2013 around 600 events have been detected and identified, 177 events with ML $\geq$ 1.5. More details about the monitoring network can be found in van Eck et al (2004) and Dost et al (2012). A first hazard analysis has been compiled by van Eck et al (2006)

In August 16, 2012 an earthquake near Huizinge, Mw = 3.6, was strongly felt and caused damage (Dost and Kraaijpoel, 2013). This earthquake is the largest observed up to now and motivated the regulator the re-assess the possible hazard in re-evaluating the extrapolation of the magnitude–frequency relation and its maximum possible earthquake. Moreover, it initiated a significant re-evaluation of the possible hazard due to induced seismicity.

2. BACKGROUND

The estimation of seismic hazard assumes the capability to predict the probability of the exceedance of a specific ground motion level. This is only possible if we can adequately model the occurrence of earthquakes. For natural, tectonic seismicity the occurrence can be described as a stationary Poisson process. Induced seismicity, however, depends on non-stationary processes such as gas production. As a result, the seismicity itself is inherently non-stationary. So far we did not find a methodology to correlate convincingly the gas extraction production process with induced seismicity. In lack of a better, but more complex hazard estimation model, we choose to vary a simple model with possible input variations, but still assuming stationary seismicity models. This would imply that may have to adapt the hazard estimations with time when new and more knowledge becomes available.

In 2004 it was assumed a stationary process for the seismicity to following a nearly stationary production rate. Today we conclude that the production rate is not stationary (Fig 2.1). In a model in which we define stationary seismicity in limited time intervals we may identify the August 16, 2013 as a second break in the stationary rate of seismic energy release, i.e. seismicity. Up to now seismic hazard model included

different models to estimate the impact of variations in seismicity rate and maximum magnitude on the hazard estimates.

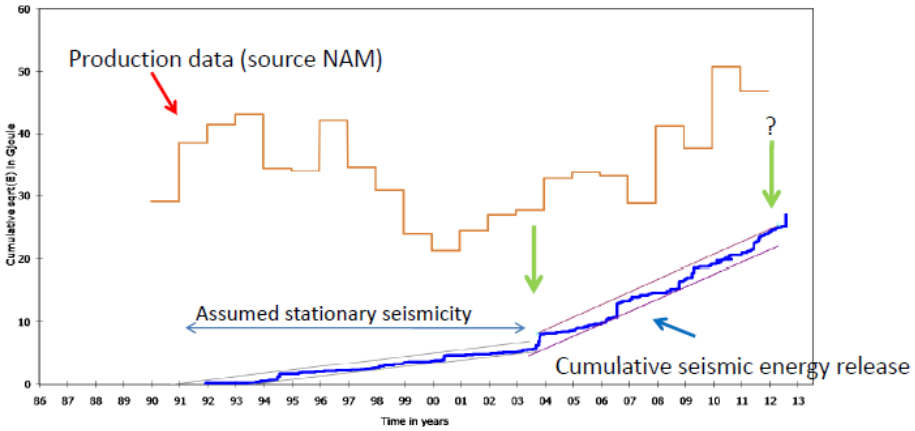

Figure 2.1 Production rate and cumulative seismic energy release versus time (in years)

3. PSHA

A PSHA (Abrahamson 2006; Cornel, 1968; McGuire and Arabasz, 1990, McGuire, 1995; Reiter, 1990) was used to calculate hazard maps. The PSHA combines at one site the hazard contributions from all potential earthquake sources below and around the site. In this model earthquakes occur in seismogenic zones characterized by earthquake rate and magnitude – frequency distribution. The wave propagation effect is characterized by Ground Motion Prediction Equations (GMPE) also called attenuation functions. The PSHA can then be estimated in four steps as reported by Kramer (1996):

1. Identification and characterization of the probability distribution of the potential rupture locations capable of producing significant ground motion at the site. In most cases, uniform probability distributions are assigned to each zone, implying that earthquakes are equally likely to occur at any point within the source zone. These distributions are then combined with the source geometry to obtain the corresponding probability distribution of source-to-site distance.
2. Characterization of the temporal distribution of earthquakes recurrence. A recurrence relationship, which specifies the average rate at which an earthquake of some size will be exceeded, is used to characterize the seismicity of each source zone.
3. Estimation of the ground motion produced at the site by earthquakes of any possible size occurring at any possible point in each source zone. Usually empirically obtained Ground Motion Prediction Equation are used. The uncertainty inherent in the predictive relationship is also considered in a PSHA.
4. Combination of the uncertainties in earthquake location, earthquake size, and ground motion parameter prediction to obtain the probability that a specific ground motion parameter will be exceeded along a particular time period.

The hazard for each point of our map is obtained by computing (numerically) the hazard integral (Cornell, 1968; Bazzurro and Cornell, 1999) for different threshold values A_0, providing the mean annual rate of exceeding of the threshold value A_0:

$$\sum_{i=1}^{N} E_i(A > A_0) = \sum_{i=1}^{N} \lambda_i \left\{ \int_M \int_R \int_\varepsilon P[A > A_0 | m, r, \varepsilon] f(m) f(r) f(\varepsilon) \, dm \, dr \, d\varepsilon \right\}_i \qquad [1]$$

Where P represents the conditional probability of exceeding a threshold value (A_0) of a ground-motion parameter (A) for a given magnitude (m) distance (r), and ε represents the residual variability of A with respect to the selected ground motion prediction equation (GMPE). The function P represents the probability of exceeding value A_0 for a given triplet m-r-ε. The probability density functions (PDFs) of magnitude M, f(m), distance R, f(r) and ε, f(ε) depends, respectively, upon the adopted earthquake recurrence model (e.g., Gutenberg and Richter, 1944), the source geometry and the selected GMPE. Finally, α_i for each zone is the mean annual rate of occurrence of earthquakes with magnitude greater than some specified lower bound.

4. HAZARD MODELLING

Input parameters should describe where the seismicity occurs (seismic zonation), characterize the seismicity (rate, magnitude-frequency relation and bounding magnitudes – max and min) and ground motion prediction equations (GMPE).

4.1 Seismic zonation

The seismic zone was defined largely by the gas reservoir area projection on the surface. The

assumption that seismicity can occur in this whole region at a depth of about 3.0 km was made. Two seismic zonation models were prepared: a single-zone model with uniform distribution of seismicity and a four–zone model with a piecewise uniform distribution of seismicity. This last choice of zonation has been motivated by a subjective interpretation of the seismicity, reservoir behaviour and geology (Petroleum Exploration Society of Great Britain, 2011; NIAG-TNO, 2004).

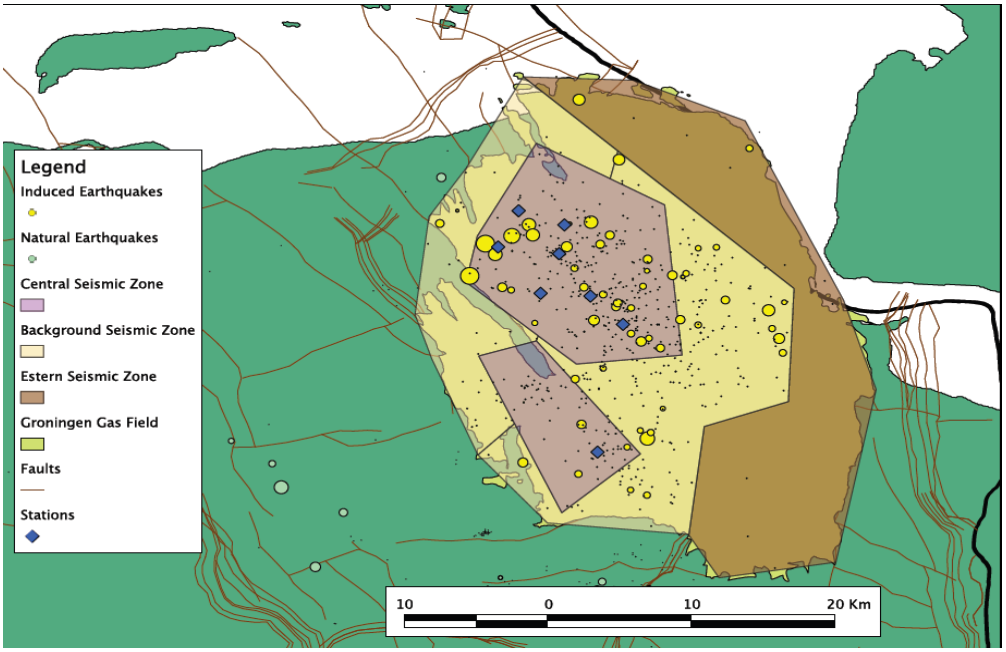

Figure 4.1. Seismic zonation of the Groningen reservoir with the past (induced) seismicity.

4.2 Seismic characteristics

Seismicity was characterized largely by the exponential magnitude frequency relation (Gutenberg and Richter, 1944). The observed earthquakes seem to follow fairly well this simple model and a more complex model does not seem to be required. The function is defined as (McGuire and Arabasz, 1990):

$$\lambda_m = e^{(\alpha-\beta m_{min})} \frac{e^{(-\beta(m-m_{min})} - e^{(-\beta(m_{max}-m_{min})}}{1 - e^{(-\beta(m_{max}-m_{min})}} \quad [2]$$

In which λ_m is the mean annual rate of exceeding a magnitude m earthquake. The other parameters are related to the a and b values in the magnitude frequency relation. The function specifically defines magnitude cut-off's at low (M_{min}) and high magnitude (M_{max}).

4.3 Magnitude cut-off

The lower magnitude cut-off has been chosen at M = 1.5. This is below the magnitude level for which people feel the earthquake (around 1.8) and corresponds to the magnitude of completeness for the local network.

The upper magnitude level has been estimated at different levels: M = 4.0, 4.5 and 5.0. This indicates different levels of conservatism with regard to the occurrence of future earthquakes.

M_{max} has been modified independently, but not between source zones.

4.4 Seismicity rate

The seismicity rate is an important model parameter for estimating different hazard scenarios.

From Figure 2.1 we assume an increased seismic energy release, i.e. rate of seismicity around 2013. Therefore we assume a future higher rate of seismicity after 2012 - 2013. Here λ is the number of earthquakes per year with magnitude equal or higher then M = 1.5

The four-zone model, as depicted in Figure 4.1 has different seismicity rates associated with each zone. The b-values, however, have been kept constant for all zones, because up to now there are no indications for specific variations.

The individual seismicity rates were defined from the past observed seismicity in the different zones. Visually it is already recognizable that some zones have a denser seismicity then others (Figure 4.1). An annual estimation of the relative rate for each zone was performed from the observed seismicity during the period 2004 – 2012. The obtained models are presented in Table 4.1a and b and in Figure 4.2). The seismicity rate for each zone was modelled with a best fit power law equation to observed seismicity (2004 – 2012) in each region and extrapolate to the period 2004-2017 as seen in Tab. 4.1b and Fig.5.2.

Table 4.1a Seismogenic zones parameterization

Seismogenic zone	Source depth (km)	b	M_{max} (Mw)	Surface area (km^2)
Background	3.0	1.08	4.0/5.0	427.55
Eastern area	3.0	1.08	4.0/5.0	370.50
Central North	3.0	1.08	4.0/5.0	214.08
Central South	3.0	1.08	4.0/5.0	84.87
Total				1097

Table 4.1b Annual seismicity rate

Seismogenic zone	2004	2005	2006	2007	2008	2009	2010	2011	2012	2004 - 2012	2004 - 2017
Background	1	1	1	0	5	2	5	11	6	3.56	4.88
Eastern area	0	0	0	0	0	0	0	0	1	0.11	0.0
Central North	4	9	13	7	4	14	6	11	9	8.56	8.56
Central South	1	1	2	2	1	0	3	1	0	1.22	1.21
Total	6	11	16	9	10	16	14	23	16	13.44	14.65

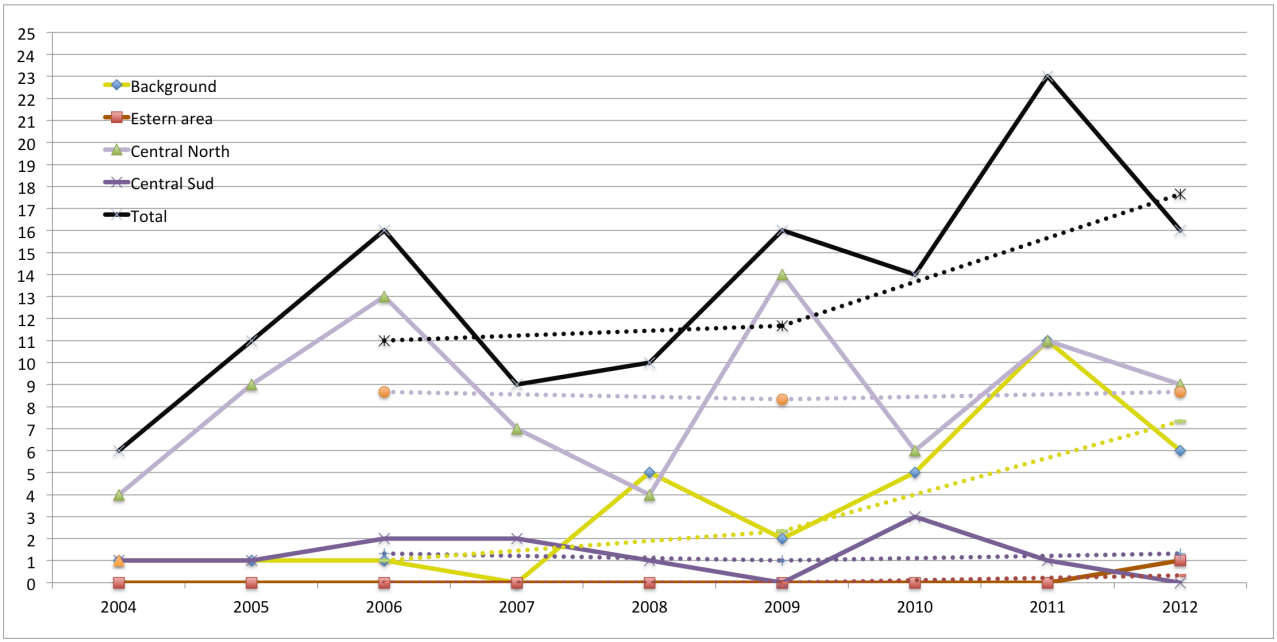

Figure 4.2 Annual seismicity rates for different seismogenic zones (different colour) and the annual total seismicity rate (black). The dashed lines represent the same quantity evaluated with time windows of three years.

4.5 Ground Prediction Equations (GMPE)

The PSHA was performed for PGA and PGV values using three different GMPE's, i.e., Campbell-97 (Campbell, 1997), Dost-04 (Dost et al.,2004) and Douglas-13 (Douglas et al.2013). A comparison with the observed data is shown for M = 3.6 in Figure 4.3a and b. Both last equations include data from shallow (induced) events in The Netherlands. They also have relatively large uncertainty bounds, Douglas-13 larger than the Dost-04. Furthermore Dost-04 has been extrapolated beyond 20 km for which no data has been available.

The differences between the two GMPE's including data from The Netherlands in terms of standard deviation (σ) and mean values are more evident in terms of probability of exceedance for a fixed value of magnitude and distance $P[A \geq A_0|M,R]$, as can be seen from Figure 4.4.

Another implication of the different uncertainty estimates is that the Douglas-13 GMPE resulted in larger probability values than the Dost-04 GMPE for a high value acceleration or velocities. This is, for example, illustrated in the PSHA by higher hazard

levels with low probabilities for Douglas-13(Figure 4.6).

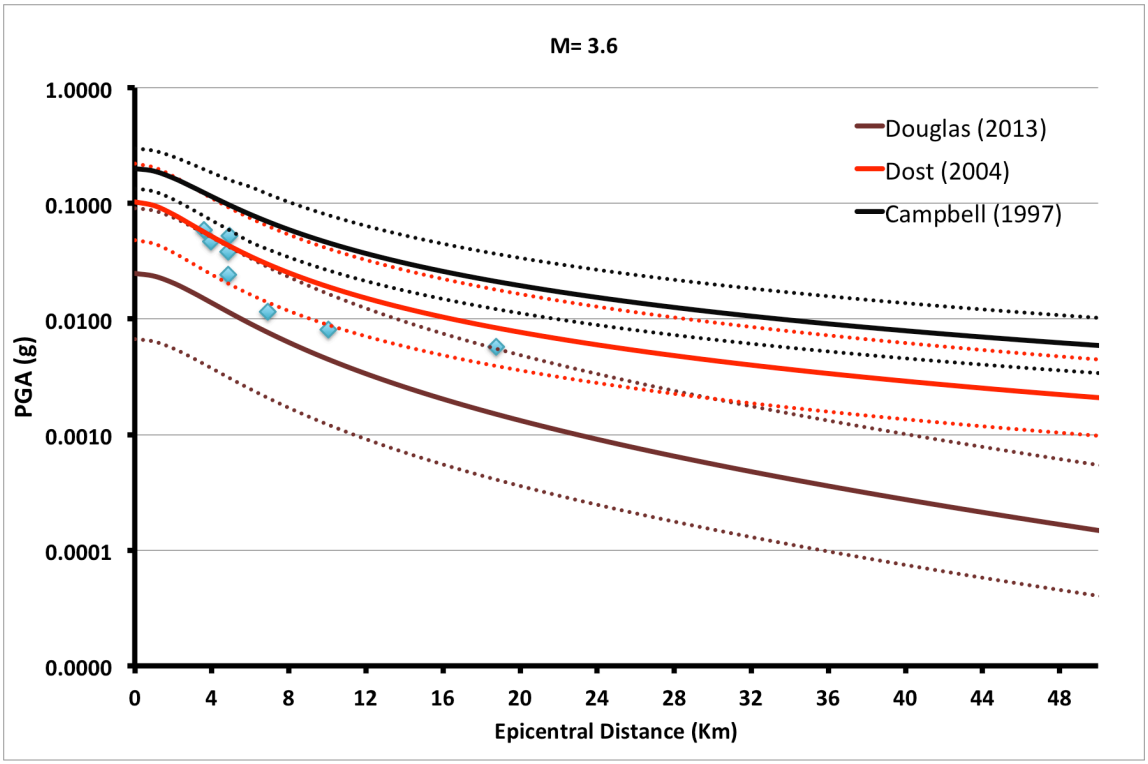

Figure 4.3a Ground motion prediction equations used for the PSHA. PGA value estimates, mean and ± one standard deviation for the GMPE obtained by Campbell (1997), Dost et al (2004) and Douglas et al (2013). Inserted dots are observed values for the August 16, 2012 earthquake.

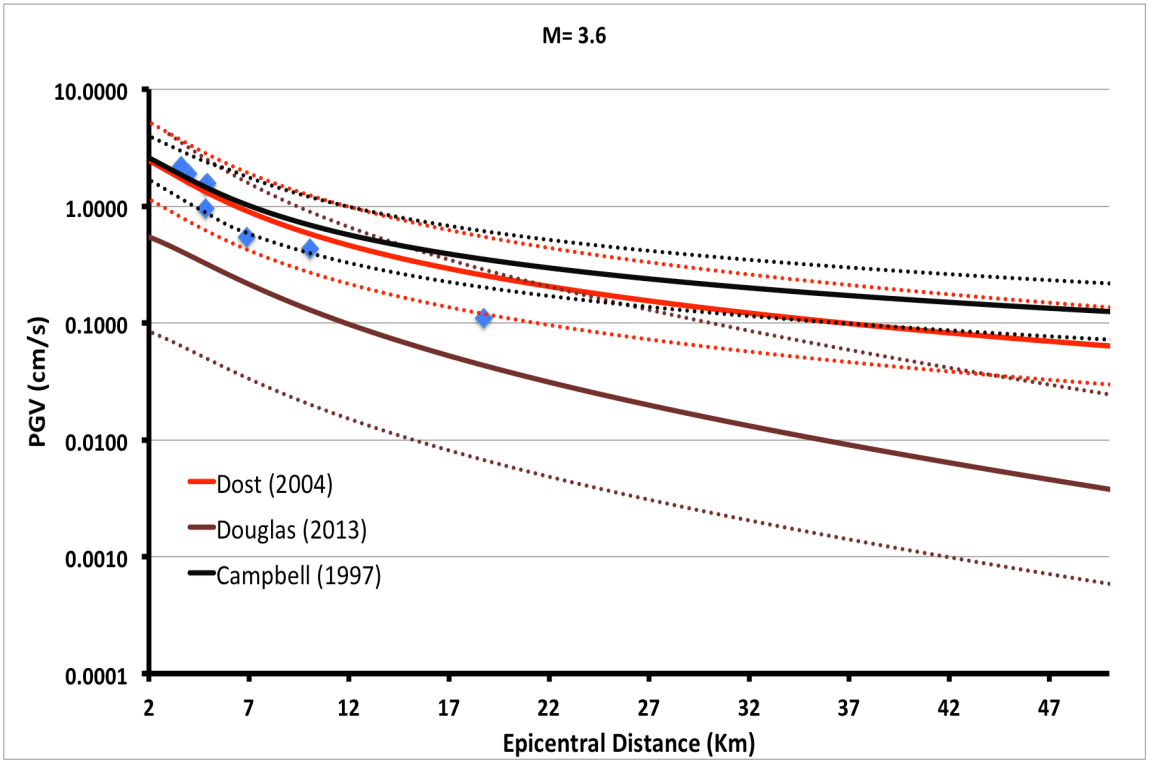

Figure 4.3b Ground motion prediction equations used for the PSHA. PGV value estimates, mean and ± one standard deviation for the GMPE obtained by Campbell (1997), Dost et al (2004) and Douglas et al (2013). Inserted dots are observed values for the August 16, 2012 earthquake.

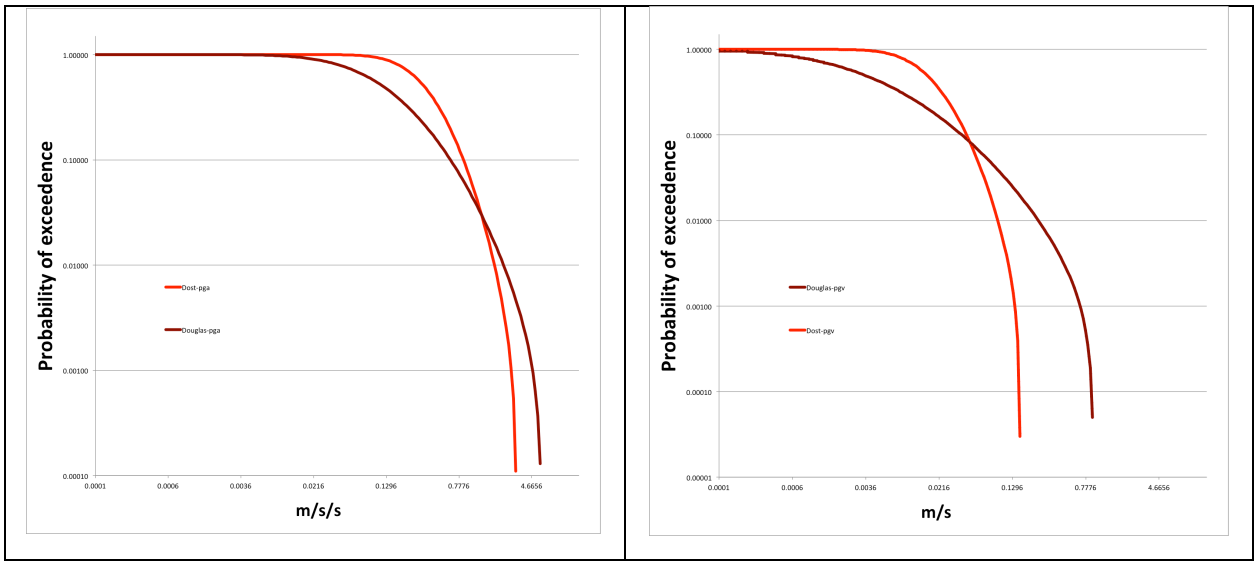

Figure 4.4 Probability of exceedance for PGA (left) and velocity (right) for the two GMPE's of Dost et al (2004) in red and Douglas et al (2013) in black.

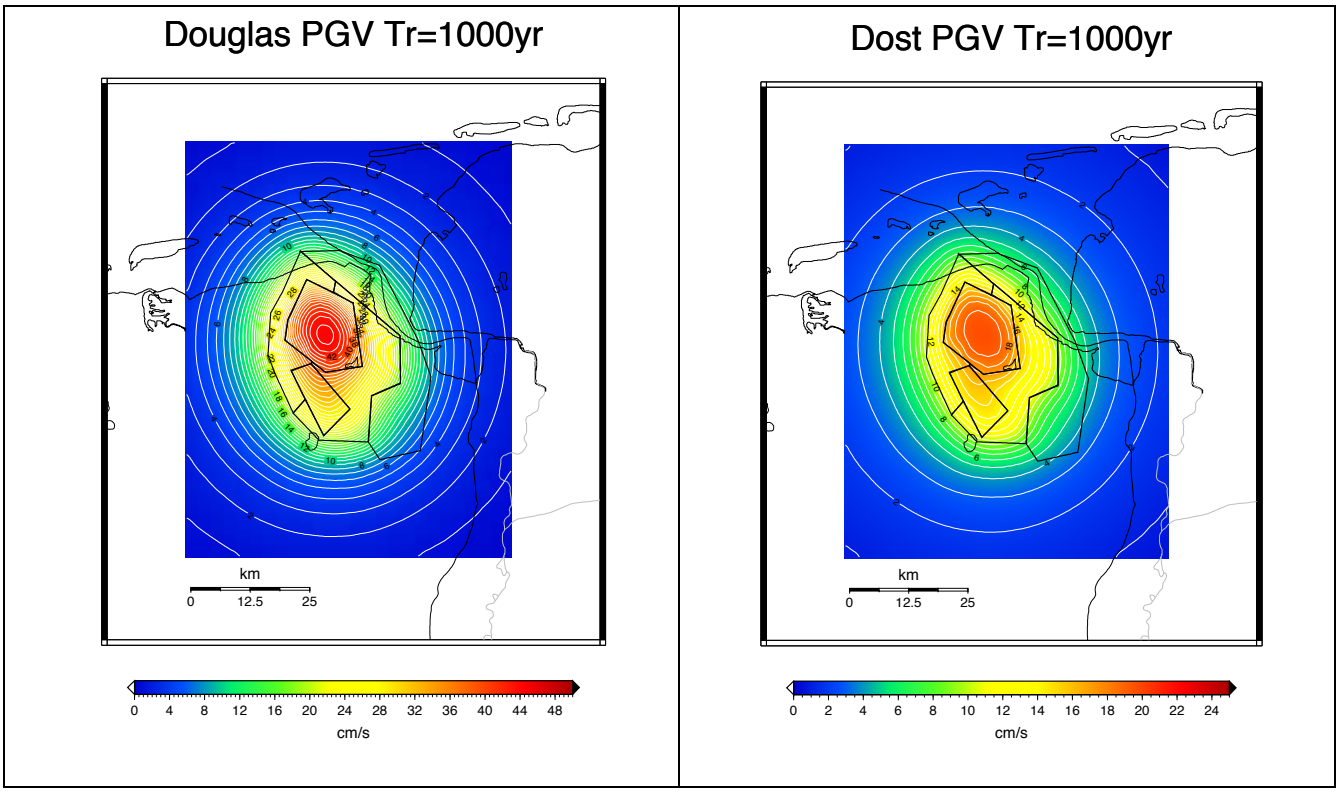

Figure 4.6 Hazard estimates for Peak Ground Velocities (PGV) with low probabilities (i.e. return period of 1000 years). A comparison between the Douglas et al (2013) GMPE and the Dost et al (2004) GMPE. The large uncertainty associated with the first relation results in higher hazard with low probabilities.

5. PSHA RESULTS

The hazard map for Groningen has been estimated using the PSHA approach for a grid of 945 points in and around the surface projection of the Groningen gas field (see Figure 5.1). The maximum distance of 50 km was considered to calculate the PGA and the PGV. The magnitude range considered was [1.5, M_{max}], with M_{max} varying in different models from M_{max} = 4.0, 4.5 and 5.0. For sake of brevity we display only the results obtained for PGA, M_{max}=5.0 using Dost-04. Additional details about the grid and integration steps are reported in Table 4.1.

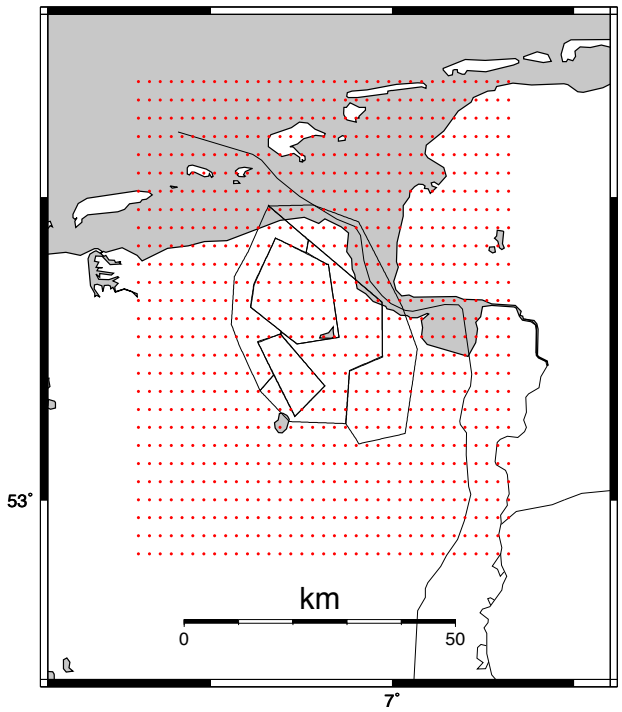

Figure 5.1 Hazard estimation grids indicating the points for which the PSHA has been done. using different model parameters.

Table 4.1 Details on the grid of points for which the PSHA has been done and on which the contour plots in the following sections are based (top), and the numerical steps for which the hazard integration was performed (bottom). Δx, Δy grid intervals in degrees; ΔR – distance integration step in km; ΔM – magnitude integration step; Rmax – maximum distance considered

Grid configuration	
Δx	0.03°
Δy	0.03°
No of grid points	945
Latitude range	52.91-53.69
Longitude range	6.3-7.32

Hazard Integration Parameters	
ΔR	1.0 Km
ΔM (Magnitude)	0.5
Rmax	50.0 Km
Return periods	50, 95, 475, 1000

A conservative hazard estimate has been obtained by choosing a high M_{max}. Other variables, like GMPE and zonation model, have been varying (for sake of brevity only the results obtained for PGA, M_{max}=5.0, and Dost-04 are reported).

For the single-zone zonation model, with a uniform spatial distribution of earthquakes, a hazard up to 0.26g for 10% probability in 50 years was observed. For the four zone model we obtain a hazard up to 0.34g for a 10% probability in 50 years.

For a shorter time window (10% probability of exceedance in 10 years) the results are reported in Figure 5.2 using different time windows to evaluate the seismic rate.

5. DISCUSSION AND CONCLUSIONS

The seismic hazard due to induced seismicity was evaluated for the Groningen gas fields where we observe a time-depended seismicity. We aim to address the problem of seismic hazard estimation given seismicity rate changes that seem to be associated with changes in production. A classical PSHA approach was adopted to calculate a set of hazard maps, varying the seismicity characteristics input model. In one experiment we assume stationarity only within different specified time windows. The time distribution of λ in combination with the four zonation allowed us to evaluate the space and time hazard variation.

In another experiment a power law equation for λ was estimated for each seismic zone, using the discrete time distribution of λ. The definition of the λ(t) equation allow us to estimate a seismicity rate in the period 2004-2017 and thus use it to evaluate a possible hazard scenario five years ahead.

We obtain time varying seismic hazard estimates that may reflect the observations. However, we still need to corroborate these preliminary results with actual observations.

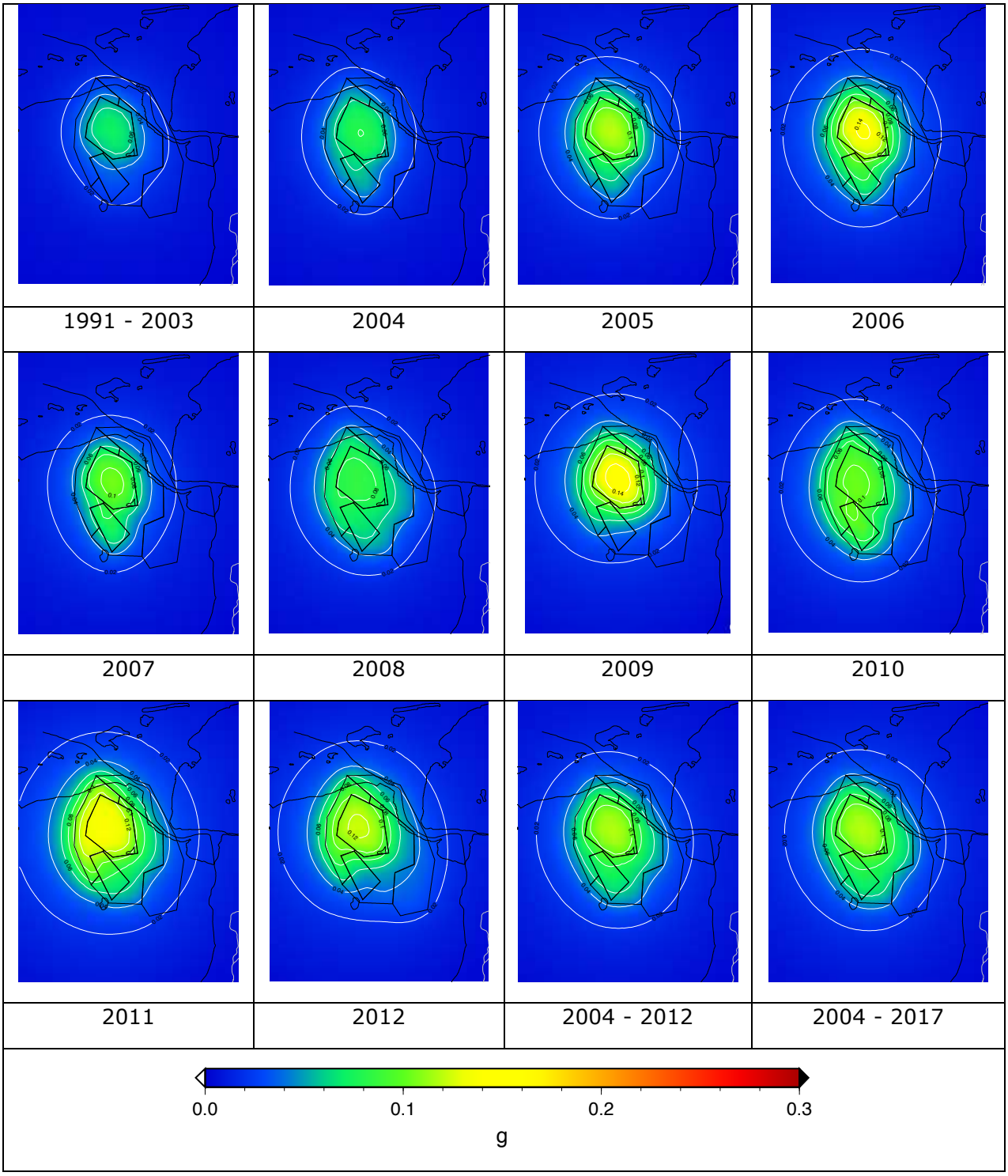

Figure 5.2 Hazard map estimates for probability of exceedance of 10% in 50 years. The seismicity rate used to calculate the map was evaluated in the time period reported below the each map.

REFERENCES

Abrahamson, N.A., "Seismic Hazard Assessment: Problems with Current Practice and Future Developments," Proceedings, First European Conference on Earthquake Engineering and Seismology, Geneva, Switzerland, September 2006, 17 pp.

Campbell, K. W. (1997), Empirical near-source attenuation relationships for horizontal and vertical components of peak ground acceleration, peak ground velocity, and pseudo-absolute acceleration response spectra, Seismological Research Letters, 68(1), 154 -179.

Cornell, C. A. (1968). Engineering seismic risk analysis, Bull. Seismol. Soc. Am. 58, 1583–1606.

Dost, B., T. Van Eck and H. Haak, 2004, Scaling of peak ground acceleration and peak ground velocity recorded in the Netherlands, Bollettino di Geofisica Teorica ed Appliocata, 45,3: 153-168.

Dost B., F. Goutbeek, T. Van Eck, D. Kraaijpoel, 2012, Monitoring induced seismicity in the North of the Netherlands: status report 2010, KNMI-REPORT January 2012

Dost B., D. Kraaijpoel, 2013. The August, 16 2012 earthquake near Huizinge (Groningen). KNMI-REPORT January 2013.

Douglas J. et al., 2013, Predicting ground motion from induced earthquake in geothermal areas, submitted to Bull. Seismol. Soc Am.

Gutenberg, B. and Richter, C. R. (1944). Frequency of earthquakes in California, Bull. Seismol. Soc. Am. 34,185–188.

Kramer S. L., 1996. Geotechnical earthquake engineering. Prentice-Hall Civil Engineering and Engineering Mechanics Series, Upper Saddle River, NJ: Prentice Hall,| c1996

McGuire, R. K., 1995. Probabilistic Seismic Hazard Analysis and Design Earthquakes: closing the Loop. Bull. Seismol. Soc. Am., 85, 1275 – 1284.

McGuire, R.K., and Arabasz, W.J., 1990. An introduction to probabilistic seismic hazard analysis, in S.H. Ward, ed. Geotechnical and Environmental Geophysics, Society of Exploration Geophysicists, Vol. 1, pp. 333-353.

NIAG-TNO, 2004. Geological Atlas of the subsurface of The Netherlands – onshore. 103 pp.

Petroleum Exploration Society of Great Britain (2011).

Reiter, L., 1990.Earthquake Hazard Analysis: issues and insights, Columbia University Press, 254 pp.

Van Eck T., F. H. Goutbeek, H. Haak, B. Dost., 2004, Seismic hazard due to small shallow induced earthquakes, KNMI, Scientific report; WR 2004-01.

Van Eck T., F. H. Goutbeek, H. Haak, B. Dost., 2006, Seismic hazard due to small-magnitude, shallow-source, induced earthquakes in The Netherlands, Engineering Geology, 2006, 87, 105-121, doi:10.1016/j.enggeo.2006.06.005.

Acknowledgements

This study was partially funded by GEISER (Geothermal Engineering Integrating Mitigation of Indued Seismiity in Reservoirs) projet funded under contrat 241321 of the EC-Researh Seventh Framework Programme (FP7).